Some Advances in Design Representation and Feasibility Analysis

David Kazmer
University of Massachusetts Amherst

Liang Zhu
University of Massachusetts Amherst

Christoph Roser
Toyota Research Laboratories

Abstract
A design representation has been developed that derives the feasible decision set from defined specifications and linear performance functions. This representation allows the design team to rationally choose a design concept and dynamically improve the design. Several applications of the representation are reviewed. Current research utilizing the representation is exploding in diverse directions: 1) developing improved Simplex-like algorithms for efficient feasibility analysis, 2) extending the representation to non-linear systems, 3) modeling of uncertainty and flexibility during development, and 4) incorporating preference functions for design optimization.

Key Words
Design representation; decision based design; axiomatic design; process window; feasibility analysis.

Objective
The objective of current research is to enable a design representation that captures the engineering specification, customer preferences, mechanistic behavior, and designer decisions. It is desired that this representation evolve dynamically throughout the development cycle, improving in fidelity and reducing uncertainty with additional information. The representation should provide support for rational design decisions: modeling the feasibility of different concept designs and driving the design towards true optimality in the layout and detailed design stages.

A second objective of current research is to provide linkages between the developing representation and other prevalent design methodologies. In the long term, a rational design methodology is sought that integrates key elements from decision based design, Taguchi design, axiomatic design, design of experiments, and others. Ultimately, the developed methodology will be accessible to and accepted by practicing engineers through simple software tools.

Approach
The current research approach is to establish a feasibility map based on the known system behavior and extreme allowable constraints of the design. Different design concepts with major variance in system topologies and behaviors can individually be modeled. Once the global feasible space has been estimated, many design decisions can be made based on performance, uncertainty, flexibility, cost, etc.

The feasibility map, or design and/or process window (domain dependent), can be generated from a set of specifications and prediction models. The prediction models, which relate controlled product and process variables to

product quality attributes, may be derived from analysis, experience, and/or experiments utilizing design of experiment or response surface methods. These prediction models typically have the form:

$$y_i = f_i(x_1, x_2, x_3, ..., x_n) \quad (1)$$

Denoting the i^{th} quality attribute as y_i, a typical specification can be expressed as $LSL_i \le y_i \le USL_i$. In many cases, the quality attribute is a one-sided constraint. Then the specification becomes $LSL_i \le y_i$ or $y_i \le USL_i$. It is not trivial to define the proper specification limits due to the potential conflict among the multiple quality attributes. Working with the development team, the product and process engineer may jointly update the specification limits during an iterative development process.

The details of the algorithm for mapping the product/process feasibility are available [1, 2]. Essentially, the algorithm is a three-step process: 1) combinatorial sub-system generation; 2) analysis of permuted constraints; and 3) resolution of extreme points. Each of these steps will be briefly described.

Sub-System Generation: Consider a system consisting of *n* design or process control variables and *m* quality attributes. The extreme limits of the feasible process are formed by the boundary of one or more active constraints in the defined system. The key to finding feasibility boundary, then, is to establish the critical constraint combinations for the system. The first step in the solution requires the generation of a list *z*, composed of *n* elements of *x* augmented with *m* elements of *y*:

$$z = \{x_1, x_j, \cdots, x_n, y_1, y_i, \ldots, y_m\} \quad (2)$$

A k-subset [3] is then defined consisting of exactly C^n_{n+m} elements, where

$$C^n_{n+m} = \frac{(n+m)!}{n!\,m!} \quad (3)$$

This set represents all possible combinations of the control variables, *x*, with the quality attributes, *y*. For four control variables and three quality attributes, a set of thirty-five sub-systems needs to be analyzed. For this example, Figure 1 shows a graph representing the 35 subset combinations, where $\{C_1\}=\{x_1,x_2,x_3,x_4\}$, $\{C_2\}=\{x_1,x_2,x_3,y_1\}$, and $\{C_{35}\}=\{x_4,y_1,y_2,y_3\}$.

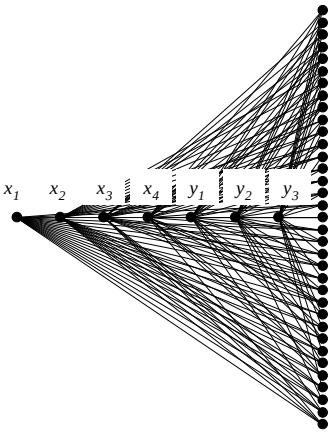

Figure 1: k-Subset of Four Control Variables and Three Quality Attributes

Analysis of Permuted Constraints: Each defined sub-system consisting of *n* variables is then analyzed for all permutations of the defined constraints. The permutation list consists of P^2_n elements where

$$P^2_n = 2^n \quad (4)$$

This set represents the control limits and specification limits that correspond to the variables defined in the C_k subset. For the given example with four control variables, Figure 2 shows a graph of sixteen constraints is analyzed, where for $P_1|C_1=\{LCL_1,LCL_2, LCL_3,LCL_4\}$,$P_2|C_1=\{LCL_1,LCL_2,LCL_3,UCL_4\}$, …,$P_{15}|C_{35}=\{LCL_4,USL_1,USL_2,USL_3\}$, $P_{16}|C_{35}=\{UCL_4,USL_1,USL_2, USL_3\}$.

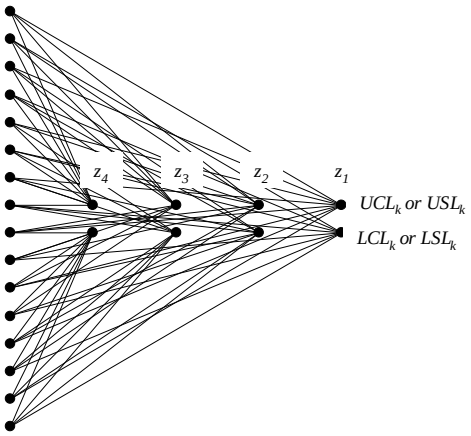

Figure 2: Permutation of Constraints for k-Subset with Four Variables

A set of extreme points is then solved for each k-subset of the system with its corresponding permutation of constraints. The number of sub-system analyses that are performed is equal to $C^n_{n+m} \cdot P^2_n$, or 35 times 16 equals 560 cases for the preceding example as represented by the graph shown in Figure 3. It should be noted that only a small number of the sub-systems that are analyzed will satisfy the feasibility requirements of all process variables and quality attributes.

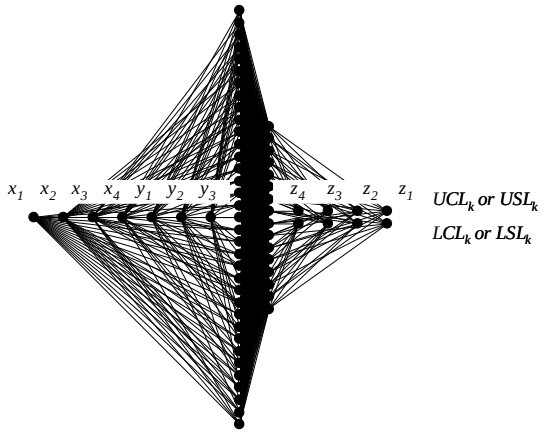

Figure 3: Graph of k-Subset Combinations and Constraint Permutations

Resolution of Extreme Points: Process engineers are interested in both the global feasible set of process conditions and quality attributes. The global feasible set of process conditions has been termed the decision space, since decisions are made about the processing variables to achieve the quality attributes. The global feasible set of quality attributes has been termed the performance space, since the performance of the process is ultimately measured by the quality and cost of the manufactured product. The described algorithm solves both of these spaces.

The result of the preceding analysis is an exhaustive set of processing conditions and their resulting quality attributes, where each set corresponds to one solution of a derived subsystem. Only a subset of these points lay on the extreme feasible boundary of the global system. Continuing with the previous example, Figure 4 plots a set of 560 points in the performance space (quality attributes, y_i) corresponding to the solution of all k-subset combinations and constraint permutations.

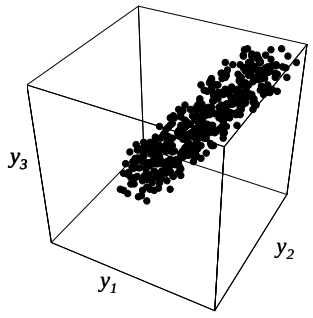

Figure 4: Extreme Points from All Subsystems

For linear system models, convexity properties significantly simplify the solution of the global feasible space. Based on the convexity, the decision space and the performance space are the convex hulls of the extreme points. Convex hull methods, such as qHull [4], enable the efficient reduction of potential extrema to derive the desired feasibility maps. Figure 5 plots the global feasible performance space for the preceding example. The decision space (processing variables, x_j), and a feasible space for any desired combination of processing variables and quality attributes are similarly derived from the local extrema of all subsystems.

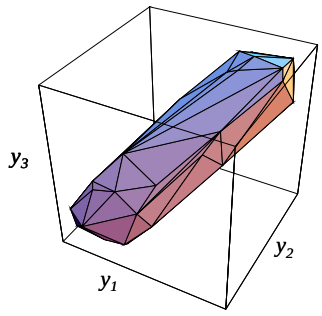

Figure 5: Global Extreme Points for System

The set of extreme points can be utilized for vital process interpretation by returning from the space representation to the graph representation. Figure 6 is a graph of the k-subset combinations and constraint permutations from Figure 3 where all non-extreme subsets have been removed. The set has been reduced from 560 subsystems to 16 subsystems. Though difficult to inspect the static image, the graph representation provides vital information about the trade-off between process variable and multiple quality attributes. Figure 6, for example, indicates that x_3 is never critical to changing the quality attributes. Detailed inspection also indicates that the lower specification limits on y_2 and y_3 are never critical. Such information is useful in specification development, process design, and process set-up.

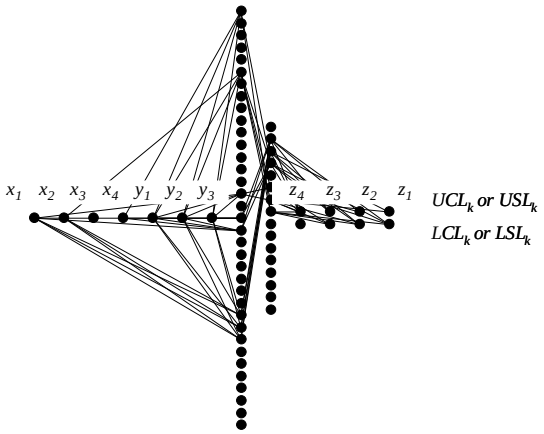

Figure 6: Graph of k-Subset Combinations and Constraint Permutations

Discussion: The feasibility maps are useful since they provide quantitative bounds on process variables and quality attributes from system models. The methods allow the process engineer to explicitly examine the trade-off between multiple quality attributes, or to compensate for a change in a processing variable by changing other processing variables. Alternatively, the process engineer may decide to hold certain processing variables and/or quality attributes fixed, and selectively examine the effect of remaining processing variables on the possibly reduced range of quality attributes.

Like most practical problems, the exploration of the global feasible space is a high-order polynomial or NP problem. The C^n_{n+m} constraint combinations dominate the polynomial order of the calculation time. However, a lower-upper decomposition [5] adopted in the algorithm has decreased the number of the linear system equations from C^n_{2n+2m} to C^n_{n+m}. Moreover, the left hand side corresponding to the coefficients of the k^{th} subsystem only needs to be inverted once for each set of permuted constraints. When the number of quality attributes is under 10, the solution requires negligible computation time. Numerical methods, such as Monte-Carlo simulation, have been implemented for validation purposes and shown to require orders of magnitude greater computational time for reduced accuracy.

Accomplishments

The design representation has been completed for linear systems. Currently, further research is investigating improved Simplex-like algorithms for efficient feasibility analysis, which is necessary for analysis of larger systems and discreet, non-convex multi-linear systems. If successful, computational geometry approaches can be utilized to extend the representation to non-linear systems by modeling the feasible volumes in high dimensional spaces. Significant and very interesting research is also investigating the

use of the representation, specifically the handling of uncertainty throughout the development cycle as the design and the design model improve. This research is leading directly to approaches for considering controllability, coupling, and flexibility in design. Moreover, concepts from multi-attribute utility theory are being considered to allow the modeling and incorporation of preference functions for design optimization with minimal information and overhead requirements. Finally, these resulting estimates of design feasibility and utility can be utilized as a performance measurement for the efficient derivation of optimal design of experiements.

While the diverse and challenging nature of the current research may suggest lack of significance in past accomplishments, the true value of the research is established through completed applications using the linear representation:

Comparison of decision and constraint based design: Beam design has been widely used as an engineering problem to demonstrate multiattribute design methods. A schematic picture of a beam structure and its design parameters are given in Figure 1. This application is part of an airframe design with the cyclic loading P and Q. Assuming that Aluminum 2024-T3 is used, the permissible maximum stress of the material corresponding to 10^7 cycles, σ_{per}, equals 124MPa, and its Young's Modulus, E, equals 72.4GPa. The case study was solved with constraint-based reasoning and decision based design approaches utilizing the described representation.

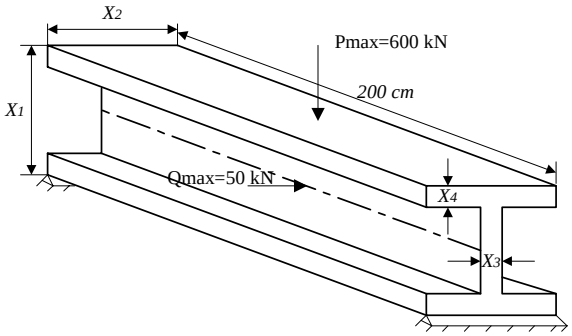

Figure 1. Beam Design

Three attributes, cross section area y_1, static deflection y_2, and maximum stress y_3 are specified to measure the overall performance. The performance attributes were formulated [6]. The resulting design feasibility is shown in Figure 8.

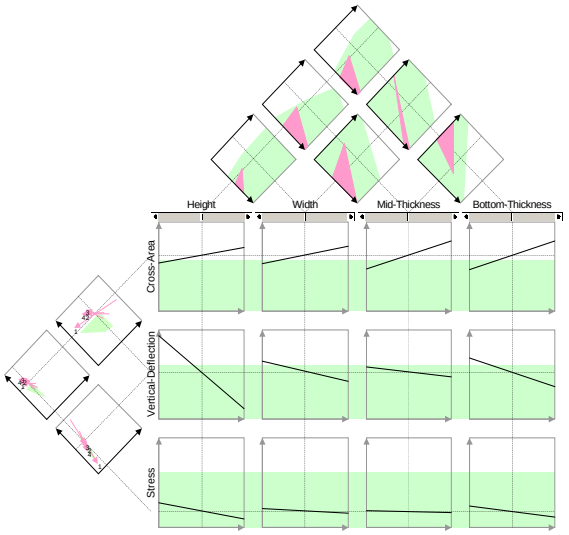

Figure 8: Constraint-Based Feasibility

In each method, the representation was used to find a feasible design, and then improve unsatisfactory performance attributes within the specification. The current design vector $X^*=(80, 39.4, 0.9, 2.57)^T$, acquired after a few steps from the first infeasible vector, gives the performance $Y^*=(313.6, 0.028, 47.2)^T$. The figure reveals that X* is a noninferior solution. Nevertheless, other noninferior solutions also exist according to different preferences on the performance attributes. Also, the design sensitivities in the Figure illustrate that the

noninferior trade-off between the cross-section area, y_1, and the vertical deflection, y_2, can be obtained by adjusting the width x_2 or the bottom-thickness x_4. For the sake of argument, it is assumed that the designer prefers a smaller area. Then the performance space leads the design vector to decrease x_2 and x_4 to $X'=(80, 30, 0.9, 2)^T$ and $Y'=(205.5, 0.045, 66.5)^T$. Similarly, the approach can be applied to each mutual space to acquire the desired overall performance.

The constraint based method adopted a typical systematic approach in which the designer defines the performance attributes first, and then sets a specification for each attribute. Generally, these specification limits are selected by the designer without complete knowledge of the design problem. Such a design approach is criticized as lacking a rational basis, though it is commonly used.

As such a decision-based approach was also used which presents another formulation of the beam design, which replaces the performance attributes (area, deflection and stress) with final decision attributes (profit and risk). Thus, the design objective is to maximize the profit of the beam application and minimize the risk of product failure. The resulting feasibility is shown in Figure 9.

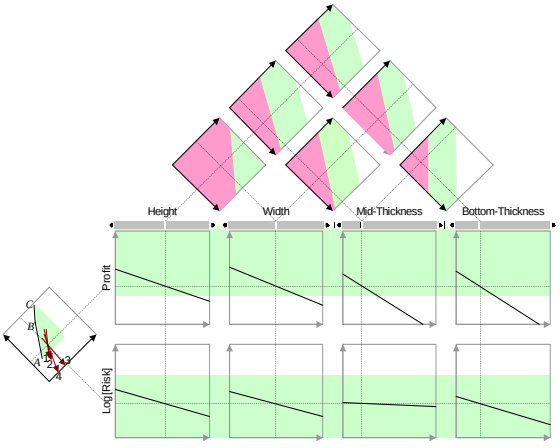

Figure 9: Decision Based Feasibility

The boundary in the risk-profit space constitutes the Pareto Optimal set. The extreme points A, B, and C respectively corresponds to three performance attributes (13%, $4\cdot10^{-8}$), (65%, 10^{-5}) and (98%, 0.099%). In order to maximize the profit and minimize the risk, any design alternative on ABC will be an "Optimal" solution. Since high reliability is expected for the airframe design, the designer is likely to select a solution closer to the point A. Utilizing the assistance of the performance space, a final design alternative may be selected as $X=(80, 44.4, 0.9, 2)^T$ with 27.6% profit and $2\cdot10^{-7}$ risk to fail during its 10^8 life cycles. Alternatively, if the main purpose of the design is to capture the maximum profit, the designer would probably choose another higher risk and higher profit option.

Figure 10 provides a comparison of the beam designed by the constraint based reasoning and decision based approach. It is noted that the design solution in Figure is only one element of the Pareto Optimal set for each of the two approaches. The solution itself depends on how the designer chooses the trade-off of multiple attributes. Given different preferences, other beam designs would likely be selected.

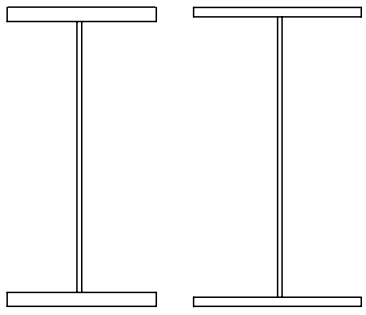

Figure 10: Comparison of Beam Designed by CBR and DBD

Development of a Process Window for Digital Video Disk Manufacturing: Injection molding is the primary manufacturing process in the creation of compact and digital video discs. Each disc is composed of an optically transparent substrate (typically polycarbonate), with one or more substrates containing a reflective metalized data surface. For prerecorded media, the data is stored on a disc in the form of pits that are molded into the disc during the injection molding process. The data is part of the disc; the data is not written in a secondary operation as in magnetic media. The bonding process combined with the small definition of data pits requires stringent flatness specifications of each DVD substrate. In addition, substrate thickness and birefringence play significant roles in the ability of the DVD laser to properly read the optical media [7-9]. The number and tightness of the quality requirements makes the DVD manufacturing process difficult to set-up.

A system model for the substrate molding process has been previously presented [10]. Consider a process with four control parameters (x_j) consisting of cooling time, first stage clamp tonnage, first stage clamp time, and second stage clamp tonnage. The quality attributes (y_i) and specifications are defined as:

$$\begin{bmatrix} -0.30 \\ -50 \\ -0.80 \\ -0.80 \end{bmatrix} < \begin{bmatrix} y_1 \\ y_2 \\ y_3 \\ y_4 \end{bmatrix} = \begin{bmatrix} \text{Min Tangential Dev} \\ \text{Max Birefringence} \\ \text{Min Radial Deviation} \\ \text{Max Radial Deviation} \end{bmatrix} < \begin{bmatrix} 0.30 \\ 50 \\ 0.80 \\ 0.80 \end{bmatrix} \begin{matrix} \text{deg} \\ nm \\ \text{deg} \\ \text{deg} \end{matrix} \quad (5)$$

Using linear regression techniques, a linear empirical model of the system was generated, along with the feasible process window shown in Figure 10.

$$\begin{bmatrix} y_1 \\ y_2 \\ y_3 \\ y_4 \end{bmatrix} = \begin{bmatrix} 0.345 & -0.021 & -0.009 & 0.058 & -0.041 \\ -19.3 & 16.0 & 0.815 & 10.1 & 0.931 \\ 0.301 & -0.095 & -0.0002 & 0.130 & -0.036 \\ 0.117 & -0.142 & 0.0217 & 0.047 & 0.023 \end{bmatrix} \begin{bmatrix} 1 \\ x_1 \\ x_2 \\ x_3 \\ x_4 \end{bmatrix} \quad (6)$$

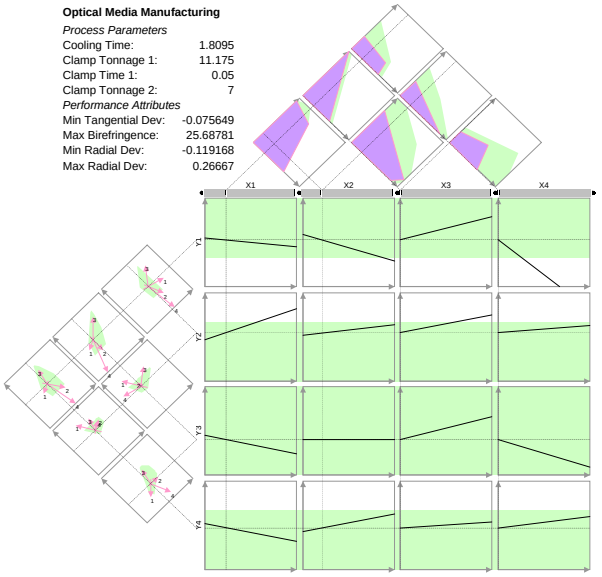

Figure 11: Feasible, Dynamic Decision Space

DVD manufacturing is a difficult challenge for the plastics industry. Given the production volumes and fierce global competition, savings of tenths and hundreds of a second in cycle time are crucial to profitability. New applications involving material, mold, or machine changes may require days of process investigations until an acceptable process settings are identified. The developed process window thus provides a method for navigating and negotiating multiple quality attributes when used by a trained process engineer.

It should be noted that each of the quality specifications have been tightened by three standard deviations from nominal to ensure 99.7% production yields with the feasible process settings as described by (Parkinson et. al., 1993). It is the goal of the process engineer to develop a robust and economic molding process. As such, the process engineer may elect to minimize the cycle time and then adjust other attributes to create a robust process. This can be accomplished by first setting x3 (stage one clamping time) to its corresponding lower control limit, then adjusting other process parameters.

Derivation of a Design/Process Flexibility Index: Assume a manufacturing process where the likelihood of setting a quality attribute to any specific value is uniformly distributed with a probability *p*. In this case, the likelihood of accepting a set of quality attributes within the specification range is:

$$\phi^{specification\_range} = \int\int_{LSL_i}^{USL_i} p dy_i = p \cdot V^{specification\_range} \quad (7)$$

where $V^{specification\_range}$ indicates the volume of the specifications, which is computed as a simple multiplication of the specification distances. Similarly, the likelihood of accepting a set of quality attributes within the global feasible space is:

$$\phi^{feasible\_range} = \oint p dy_i = p \cdot V^{feasible\_range} \quad (8)$$

where the volume of the feasible space, $V^{feasible\_range}$, can be readily computed using quick hull algorithms [4]. The process flexibility index can then be computed as a ratio of the two probabilities:

$$C_f = \frac{\phi^{feasible\_range}}{\phi^{specification\_range}} = \frac{p \cdot V^{feasible\_range}}{p \cdot V^{specification\_range}} = \frac{V^{feasible\_range}}{V^{specification\_range}} \quad (9)$$

For a uniformly distributed likelihood of quality attribute acceptance, a C_f greater than 1.0 indicates that the process is able to deliver a more diverse set of quality attributes than those defined in the specifications. This definition of the process flexibility index is not dependent on the current operating point, since the likelihood of a change is uniformly distributed.

Many quality attributes, however, are defined with just a one-sided specification. For example, part weight may have a specified maximum, or a manufactured material property may have a specified minimum. The described algorithms for computing the feasible space continue to function for such one-sided specifications; reducing the number of specifications will tend to increase the feasible space. However, the definition of the process flexibility metric is not valid for one-sided specifications, since the volume of the specification range is undefined when there is no bound for the complementary specification limit. For one-sided specifications, a weighting function is necessary to discount the likelihood of quality attribute occurring very far from the operating region. A reasonable probabilistic approach is next discussed.

The selection of the weighting function is of primary importance. Ideally, the weighting function should represent the true likelihood of process selection based on the necessary changes in the quality attributes. To accommodate inevitable shifts of the average in a process, Motorola Six Sigma guidelines have specified a $\pm 6\sigma$ production tolerance on either side of the nominal value [11]. It is commonly believed that the 6σ approach was developed to reduce the defect rate to less than three rejections per million manufactured units. However, the original motivation of the approach was to ensure a 3σ yield given a long-term 3σ shift in the mean or specifications! Based on this premise, a probabilistic approach is developed that explicitly defines the flexibility of the process.

Consider the probability density function about a current operating point as shown in Figure 8. This density function does not represent the distribution of the i^{th} quality attribute due to noise, but rather the likelihood for needing to change the i^{th} quality attribute due to external effects. As shown in the figure, there is equal probability that the quality attribute may need to be increased or decreased from the mean value, and some small probability that the quality attribute will need to be reduced below the lower specification limit.

The shaded area indicates the feasible region for this quality attribute without violating other quality attributes or requiring the process to

operate beyond its specified control limits. Using normal statistics, the probability of the process being able to accommodate changes in the i^{th} quality attribute according to the proscribed probability density function is:

$$\phi_i^{feasible\_range} = \int_{LFL_i}^{UFL_i} pdf(y_i)dy_i \quad (10)$$

where LFL_i and UFL_i are the lower and upper feasible limits for the i^{th} quality attribute, as derived from the described feasibility analysis. The likelihood for evaluating the need for a process change within the specified limits can be similarly evaluated as:

$$\phi_i^{specification\_range} = \int_{LSL_i}^{USL_i} pdf(y_i)dy_i \quad (11)$$

where LSL_i and USL_i are the specification limits for the i^{th} quality attribute. The complementary specification limit may be set to $-\infty$ or $+\infty$ for one-sided specifications. The univariate process flexibility index for both one and two sided specifications is then defined as:

$$C_f^i = \frac{\Phi^{-1}\left(\phi_i^{feasible\_range}\right)}{\Phi^{-1}\left(\phi_i^{specification\_range}\right)} \quad (12)$$

where Φ^{-1} is the inverse of the standard normal cumulative distribution, which converts the probability back to a z-score (a measure of volume very similar to equation (10)). This definition of the process flexibility is dependent upon the current operating point of the manufacturing process, since this determines the likelihood of operating outside the specification or feasible range.

A process flexibility index can be computed for each quality attribute. Since most manufacturing processes must meet multiple quality specifications, it is desirable to condense this vector of flexibility indices down to one scalar that is representative of the composite process flexibility. Several forms of multivariate indices have been proposed for process capability [12] and product robustness [13]. The multivariate index of process flexibility should reflect the combined loss if the manufacturing flexibility is insufficient to deliver multiple quality attributes. Assuming independence between changing multiple quality attributes, the joint probability of the process delivering needed changes in the quality attributes within the feasible region is:

$$\phi^{feasible\_range} = \prod_{i=1}^{n} \phi_i^{feasible\_range} \quad (13)$$

The joint probability of the process delivering needed changes within defined specifications is:

$$\phi^{specification\_range} = \prod_{i=1}^{n} \phi_i^{specification\_range} \quad (14)$$

The multivariate process flexibility index may then be defined as:

$$C_f = \frac{\Phi^{-1}\left(\phi^{feasible\_range}\right)}{\Phi^{-1}\left(\phi^{specification\_range}\right)} \quad (15)$$

As the process flexibility index increases, the process is better able to significantly change the quality attributes. It should be noted that there are substantial behavioral differences between the two definitions from equations (10) and (16). While both definitions are useful, the flexibility index of equation (10) is not dependent on the current level of the quality attributes, since the likelihood of placing a quality attribute at any location is uniformly distributed. The definition of equation (16) also exhibits significant behavioral differences. Specifically, the results of this definition can be equal to or less than zero even when a significant feasible region exists. Similar to a normalized z score, a C_f of zero indicates that there is a 50% likelihood that the process will be able to deliver the desired quality attributes. Similar to the C_{pk} metric, scores of less than zero indicate that the process is increasingly unlikely to provide the desired levels of the quality attributes.

Significant research has been motivated by limitations of the injection molding process. To investigate the flexibility of the injection

molding process, a half-factorial design of experiments [14] was performed to determine the main effects between the important process parameters and three critical part dimensions in a commercial printer housing:

$$\begin{bmatrix} L1 \\ L2 \\ L3 \end{bmatrix} = \begin{bmatrix} 0.57 & -0.10 & 0.43 & 0.02 \\ 0.51 & -0.18 & 0.29 & 0.00 \\ 0.23 & -0.05 & 0.18 & 0.10 \end{bmatrix} \begin{bmatrix} Pressure \\ Velocity \\ Temperature \\ ScrewSpeed \end{bmatrix} \quad (16)$$

In this equation, the machine parameters have been scaled to the range of 0 to 1, indicative of the maximum feasible processing range for this application. The resulting coefficients of the linear model are actual changes in part dimensions (measured in mm). It should be noted that once tooling is completed, the dimensional changes available through processing are quite limited though functionally significant.

There are two significant conclusions that can be drawn from this system model. First, all three of the dimensions react similarly to changes in the process settings. Thus, the molding process is nearly fully coupled and behaves as a one degree of freedom process in which only one quality attribute is controllable. Second, the equation shows the relative effect that each of the processing variables can have on the product quality attributes. Pressure was the most significant process variable, followed by temperature, velocity, and others.

To enhance the flexibility of the molding process, dynamic valves were designed and implemented to meter the flow and pressure of the melt to the mold cavity [15]. The current implementation, named Dynamic Feed, is shown in Figure 9. The pressure drop and flow rate of the melt is dynamically varied by the axial movement of each valve stem which controls the gap between the valve stem and the mold wall. By de-coupling the control of the melt at different valve stem positions, melt control at each gate can override the effects of the molding machine and provide better time response and differential control of the melt. Each valve acts as an individual injection unit, lessening dependency on machine dynamics.

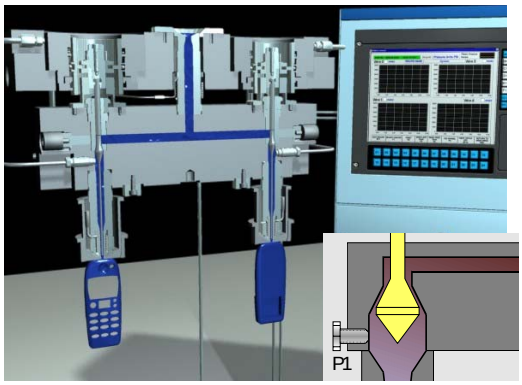

Figure 12: Dynisco HotRunner's Dynamic Feed™ System

The material shrinkage and dimensions change at differing locations in the part based on the pressure contours and histories around the gates. The ability to change individual dimensions or other quality attributes without re-tooling mold steel provides significant process flexibility. It is possible to augment equation (17) with the additional degrees of freedom and re-examine the controllability of the three part dimensions:

$$\begin{bmatrix} L1 \\ L2 \\ L3 \end{bmatrix} = \begin{bmatrix} -0.02 & -0.05 & 0.08 & -0.01 \\ -0.03 & -0.09 & 0.05 & 0.00 \\ -0.01 & -0.02 & 0.03 & 0.01 \end{bmatrix} \begin{bmatrix} Pressure \\ Velocity \\ Temperature \\ ScrewSpeed \end{bmatrix} + \quad (17)$$

$$\begin{bmatrix} 0.00 & 0.31 & 0.60 & 0.00 \\ 0.10 & 0.17 & 0.00 & 0.16 \\ 0.00 & 0.02 & 0.00 & 0.21 \end{bmatrix} \begin{bmatrix} P1 \\ P2 \\ P3 \\ P4 \end{bmatrix}$$

There are two significant implications of this result. First, the closed loop control of cavity pressures has significantly reduced the dependence of part dimensions on machine settings, as evidenced by the reduction in the magnitude of coefficients for the primary machine settings. This effect has also been evidenced by reductions in the standard deviations of multiple part dimensions by an average factor of five, resulting in an increase

in the process capability index, *Cp*, from less than 1 to greater than 2.

Utilizing the described methods, the feasible performance spaces for the conventional and new molding process are mapped in Figure 10. Using equation (10), the process flexibility for conventional molding was computed as 0.02, barely capable producing of any changes in product quality. The lack of process flexibility is a primary reason for engineering changes and delays for molded components. The process flexibility for Dynamic Feed was similarly calculated as 0.7. The greater flexibility of the new process enabled four companies to cut the time from mold design to finished part down to hours instead of weeks, as validated for five different applications in five successive days at National Plastics Exposition in the McCormick Center in Chicago [16].

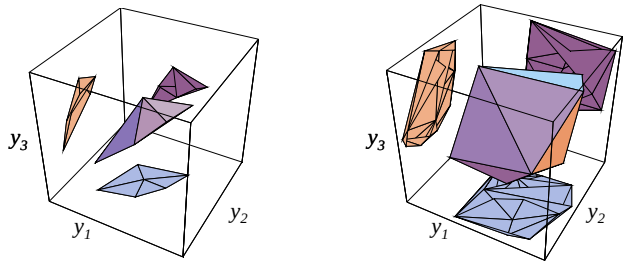

Figure 13: Feasible Performance Spaces for Conventional Molding and Dynamic Feed

Acknowledgements

This work was funded through National Science Foundation Division of Design, Manufacturing, and Industrial Innovation - grant number DMI-9702797. GE Plastics has provided funding in the robust design area related to their corporate program, Design for Six Sigma.

References

1. Kazmer, D., L. Zhu, and D. Hatch, *Process Window Derivation With an Application to Optical Media Manufacturing.* ASME Journal of Manufacturing Science, Accepted - in process.
2. Zhu, L. and D. Kazmer, *A Performance-Based Representation for Engineering Design.* ASME Journal of Mechanical Design, Accepted - in process.
3. Gross, J. and J. Yellen, *Graph Theory and Applications*. Discrete Mathematics and Applications, ed. K. Rosen. 1999, New York: CRC Press.
4. Barber, C.B., D.P. Dobkin, and H. Huhdanpaa, *The Quickhull Algorithm for Convex Hulls.* ACM Transactions on Mathematical Software, 1996. 22(4): p. 469-483.
5. Nazareth, J.L., *Computer Solutions of Linear Programs*. 1987: Oxford University Press. 231.
6. Osyczka, A., *Multicriteria Optimization for Engineering Design*, in *Design Optimization.* 1985.
7. Oshiro, T., T. Goto, and J. Ishibashi. *Experimental study of DVD substrate quality by operating conditions in injection molding.* in *Annual Technical Conference - ANTEC, Conference Proceedings.* 1997. Toronto, Canada.
8. Park, S.J., et al. *Numerical analysis of injection/compression molding process for center-gated disc*. in *Annual Technical Conference - ANTEC, Conference Proceedings.* 1998. Atlanta, GA, USA.
9. Shin, J.W., D.C. Rhee, and S.J. Park. *Experimental study of optical disc birefringence*. in *Annual Technical Conference - ANTEC, Conference Proceedings*. 1998. Atlanta, Ga, Usa.
10. Hatch, D.P., *Development of Transfer Functions for Optical Media*, in *Mechanical & Industrial Engineering.* 2000, University of Massachusetts Amherst: Amherst, MA. p. 210.
11. Feng, C.-X. and A. Kusiak. *Probabilistic tolerance synthesis: A comparative study*. in *Proceedings of the 1995 4th Industrial Engineering Research Conference*. 1995. Nashville, TN.
12. Boyles, R.A., *The Taguchi Capability Index.* Journal of Quality Technology, 1991. 23(1): p. 17.
13. Ford, R.B., *Process for the Conceptual Design of Robust Mechanical Systems going beyond Parameter Design to Achieve World-Class Quality*, in *Mechanical Engineering*. 1996, Stanford University: Stanford.
14. Luftig, J.T. and V.S. Jordan, *Design of experiments in quality engineering*. 1998, New York: McGraw-Hill. vii, 343.
15. Kazmer, D.O. and P. Barkan, *Multi-Cavity Pressure Control in the Filling and Packing Stages of the Injection Molding Process.* Polymer Engineering and Science, 1997. 37(11): p. 1865-1879.
16. DeGaspari, J., *All in a Day's Work: Teamwork by four companies cuts the time from mold design to finished part down to hours instead of weeks.* Mechanical Engineering Magazine, 2000. 122(8): p. 74-78.